

NJC

Accepted Manuscript



This is an *Accepted Manuscript*, which has been through the Royal Society of Chemistry peer review process and has been accepted for publication.

Accepted Manuscripts are published online shortly after acceptance, before technical editing, formatting and proof reading. Using this free service, authors can make their results available to the community, in citable form, before we publish the edited article. We will replace this *Accepted Manuscript* with the edited and formatted *Advance Article* as soon as it is available.

You can find more information about *Accepted Manuscripts* in the [Information for Authors](#).

Please note that technical editing may introduce minor changes to the text and/or graphics, which may alter content. The journal's standard [Terms & Conditions](#) and the [Ethical guidelines](#) still apply. In no event shall the Royal Society of Chemistry be held responsible for any errors or omissions in this *Accepted Manuscript* or any consequences arising from the use of any information it contains.

23 **Abstract**

24 A novel nano-adsorbent, magnetic carbon nanofibers (CNFs-Fe₃O₄), was prepared by
25 impregnating magnetic Fe₃O₄ nanoparticles onto the surfaces of carbon nanofibers based
26 on electrostatic interactions. The resulting nanoparticles were used as the adsorbent for
27 the magnetic solid phase extraction of polycyclic aromatic hydrocarbons from the
28 environmental water samples. The experimental parameters affecting the extraction
29 efficiency, including the amount of sorbents, desorption conditions, extraction time and
30 salt concentration were investigated and optimized. Under the optimal conditions, the
31 detection limits of the method (S/N=3) were in the range of 0.008–0.03 ng mL⁻¹ and the
32 limits of quantification (S/N=10) were between 0.025–0.08 ng mL⁻¹. Repeatability of the
33 method was assessed through five consecutive extractions of independently prepared
34 solutions at concentrations of 0.1, 10, and 100 ng mL⁻¹ of the compounds. The observed
35 repeatability ranged between 3.2–11.2% depending on the considered compounds. The
36 developed method was successfully applied to the real water samples while the relative
37 recovery percentages obtained from the spiked water samples at three level
38 concentrations (0.1, 10 and 100 ng mL⁻¹) were from 90.1 to 100.9%.

39

40

41

42 **Keywords:** Magnetic solid phase extraction; Carbon nanofibers; Polycyclic aromatic
43 hydrocarbons; Water samples.

44

45

46 **1. Introduction**

47 Polycyclic aromatic hydrocarbons (PAHs) are a class of hydrophobic organic
48 contaminants (HOC) comprised of two or more fused benzene rings. PAHs are one of the
49 most well-known classes of environmental pollutants. Some of these compounds are
50 carcinogenic and mutagenic. They are omnipresent pollutants wide in all compartments
51 of the environment (atmosphere, soil and water) and seriously dangerous to human health
52 and living organisms.¹⁻³ On the basis of their occurrence and carcinogenicity, 15 PAHs
53 have been identified as priority hazardous substances by the European Union (EU)⁴ and
54 16 PAHs by US Environmental Protection Agency (EPA)⁵, 12 of them are identical in
55 both lists. The sources of these pollutants can be created as follows: traffic pollution, oil
56 spills, volcanic activity, industrial processing and incomplete combustion of organic
57 materials.⁶ In order to reduce the human intake of these hazardous substances a chemical
58 control (and consequently methods of analysis) is required. There is a major problem for
59 the monitoring due to the very low concentrations of these compounds and complexity of
60 matrix samples.⁷ Therefore, sample preparation and preconcentration steps are very
61 necessary.

62 Solid-phase extraction (SPE) is the most common pre-treatment method for sample
63 matrix simplification and pre-concentration of trace amounts of analyte in samples.⁸
64 Recently, a new SPE technique based on the use of magnetic nanoparticles (MNPs),
65 called magnetic solid phase extraction (MSPE) has been introduced for the separation and
66 preconcentration of organic and inorganic species from complex matrixes.^{9,10} The
67 powdery magnetic adsorbent can be reversibly agglomerated and re-dispersed in solution
68 or suspensions by the application and removal of an appropriate magnetic field, thus

69 realizing the phase separation conveniently. Therefore, the time-consuming for the
70 passage of solvent through the column for desorption of the analytes and also the
71 filtration operations encountered in SPE are avoided. In addition, owing to its nano-
72 nature, MNPs possesses large specific surface area, and the equilibrium time between the
73 sorbents and also the sample solutions are thus greatly shortened, and at the end resulting
74 in relatively higher extraction capacity and detection sensitivity.¹¹⁻¹³ Among the magnetic
75 nano-sized materials, iron oxides have been extensively used as adsorbent in MSPE
76 because of their super paramagnetism, high magnetic saturation, low toxicity, simple
77 preparation process and low price. However, the drawbacks of utilizing MNPs to sample
78 preparation are their low selectivity toward the target analytes, low stability in strong
79 acidic aqueous media and low dispersion ability in various sample matrices. The stability
80 and selectivity of the MNPs can be significantly improved by the modification of the
81 surface of the adsorbent with special functional groups.

82 In recent years, a large number of carbon-based nanoparticles have been investigated as
83 sorbent materials in the sample preparation, including nanodiamonds, fullerenes, carbon
84 nanotubes, graphene, carbon nanofibers, carbon nanocones-disks and nanohorns, as well
85 as their functionalized forms.^{14,15} Recently, carbon nanofiber (CNF) has been extensively
86 studied under recognition as a unique carbon material.¹⁶⁻¹⁸ Carbon nano-fibers could be
87 defined as sp^2 -based linear filaments with a diameter of ca. 100 nm that is characterized
88 by flexibility and their aspect ratio (above 100). CNFs are hydrophobic materials with
89 ability to establish π - π interactions with our target analytes. The combination of high
90 specific area, flexibility, and high mechanical strength make them as a very attractive
91 adsorbents.¹⁹

92 As mentioned, CNFs have been considered as excellent sorbents because of their large
93 surface area and high affinity towards the various organic compounds. In the present
94 case, the CNFs were decorated with magnetic nanoparticles. As a result, the magnetic
95 CNF, which combines merits of strong adsorption property and magnetic separation,
96 should show great potential as sorbents for MSPE. In fact, the intersection of CNFs
97 science with MSPE essentially allows the proposed method to integrate the advantages of
98 both, the CNFs and MSPE. To the best of our knowledge, the use of CNFs modified with
99 magnetic Fe₃O₄ as an adsorbent has not been reported. In the present work, we prepared
100 magnetized CNFs as a new adsorbent for MSPE of selected polycyclic aromatic
101 hydrocarbons (PAHs) (naphthalene, fluorine and anthracene as model compounds) from
102 the real water samples using gas chromatography–flame ionization detector (GC–FID).

103 **2. Experimental**

104 **2. 1. Chemicals and materials**

105 Polycyclic aromatic hydrocarbons (PAHs) include naphthalene (Naph), fluorene (Flu),
106 anthracene (Anth) was bought from Merck (Darmstadt, Germany). A stock solution of
107 PAHs (500 mg L⁻¹) was prepared in the methanol and kept in a refrigerator at 4 °C. Fresh
108 working solutions were prepared daily by diluting of the stock solution in deionized
109 water. Analytical-grade ammonia, acetonitrile, ferric chloride (FeCl₃.6H₂O), ferrous
110 sulfate (FeSO₄.7H₂O), methanol, acetone, isopropyl alcohol, dichloromethane and NaCl
111 were all purchased from Merck (Darmstadt, Germany).

112 **2. 2. Instrumentation**

113 Gas chromatographic analysis was carried out using a Chrompack CP9001 (Middelburg,
114 the Netherlands) fitted with a split/splitless injector and flame ionization detector
115 (Middelburg, the Netherlands). Helium (99.999%, Sabalan Co., Tehran, Iran) was used as
116 the carrier gas and was set at 1 mL min^{-1} . The separation was performed with a CP-Sil
117 24CB (50% phenyl, 50% dimethylsiloxane) capillary column, WCOT Fused silica, 30 m
118 \times 0.25 mm ID with 0.25 μm stationary film thickness (Chrompack, Middelburg, The
119 Netherlands). The column temperature was programmed as follows: initial oven
120 temperature 70 $^{\circ}\text{C}$ for 2 min, increasing to 220 $^{\circ}\text{C}$ at 40 $^{\circ}\text{C min}^{-1}$ and holding for 15 min.
121 The injector and detector temperature were set at 250 and 280 $^{\circ}\text{C}$, respectively. A VELP
122 Scientifica heating magnetic stirrer, model ARE (Milano, Italy) was employed for stirring
123 and heating samples during the extraction. To mix various solution ingredients, a
124 ultrasonic bath (Branson 1510, Branson Ultrasonics Co., Danbury, CT), was employed at
125 a frequency of 42 kHz. Also the surface characteristics of the created coating were
126 studied by scanning electron microscopy (SEM) (LEO, model 1450VP, Germany).

127 **2.3. Procedure of magnetic solid-phase extraction**

128 Extraction was performed by adding 10 mg of CNFs- Fe_3O_4 sorbent to 50 mL of a
129 standard sample solution containing 100 ng/mL of the analytes in a glass vial. The
130 suspension was stirred for 10 min to facilitate adsorption of the PAHs on the surface of
131 sorbents. After the extraction, the magnetic adsorbents were collected by a strong magnet
132 with 1.2 Tesla magnetic field (5.0 cm \times 3.0 cm \times 2.0 cm) and the supernatant was
133 decanted. The preconcentrated target analytes were desorbed from the surface of the
134 sorbent by addition of 1 mL dichloromethane during 2 min sonication. Finally, the
135 magnet was used again to settle the nanoparticles, and the desorbed solution was

136 evaporated under a gentle nitrogen flow. The residue was re-dissolved in 50 μL methanol,
137 and 1 μL of this solution was injected into the GC system for analysis.

138

139 **3. Results and discussion**

140 **3.1. Preparation of CNFs- Fe_3O_4**

141 **3.1.1. Synthesis of branched carbon nanofiber**

142 Commercially available, unsized, polyacrylonitrile (PAN)-based carbon fibers (Toho
143 Tenax America, Inc.) were utilized as the base fiber. The carbon fibers (CFs) were
144 immersed into an iron nitrate nonahydrate solution (100 mM) and followed by ultrasonic
145 agitation for 2h. Then, they were dried and calcinated at 200°C under air flow for 2h to
146 remove the nitrate components and make the desired catalyst coating on the surface of the
147 CF. Chemical vapour deposition (CVD) was applied to grow the CNFs on the CF at
148 atmospheric pressure and the temperature at 600°C for 30min. This process was fulfilled
149 by a catalytic reaction of an acetylene flow rate of 50 standard cubic centimeters per
150 minute (sccm) over Fe/CF in the reactor under a flow rate of H_2/N_2 (100, 100 sccm). At
151 the end of the run time, the C_2H_2 flow stopped, the heater turned off and then the reactor
152 cooled under the flow of N_2 .

153 For increasing the dispersibility of CNFs into various solvents, the partially ionizable
154 carboxylic acid groups created during the oxidation of CNFs. For this reason, the
155 functionalization of CNFs was performed as follows: predetermined quantities of raw
156 CNFs (0.3 g) and 50 mL nitric acid were added into a round-bottomed glass flask, and the
157 CNFs mixture sonicated for 30 min in an ultrasonic bath. Next the mixture was refluxed
158 at 120°C and maximum stirrer rate for 24 h. After having been cooled to the room
159 temperature, the mixture was filtered on a $0.22\ \mu\text{m}$ filter (Millipore, Bedford, MA, USA),

160 washed with excess distilled water to neutral pH, and dried under vacuum at 60°C for 12
161 h.²⁰

162 **3.1.2. Preparation of surface-modified CNFs with Fe₃O₄ (CNFs-Fe₃O₄)**

163 CNFs-Fe₃O₄ NPs were prepared by a chemical co-precipitation method. In this case, 0.1 g
164 of functionalized CNFs was added to 60 mL of deionized water by ultrasonic irradiation
165 for 20 min. Then, 150 mg of FeCl₃.6H₂O and 80 mg of FeSO₄.7H₂O were added under
166 nitrogen gas with vigorous stirring for 30 min. After that, 18 mL of 25% NH₃ was added
167 to the solution until the pH of the solution reached to 11. The mixture was stirring at 80
168 °C for 1 hour. During the process, the solution temperature was maintained at 80 °C and
169 nitrogen gas was purged to prevent the intrusion of oxygen. After the reaction, the
170 obtained NPs precipitate were separated from the reaction medium by the magnetic
171 decantation, and then washed several times with deionized water until the pH became
172 neutral and finally dried.

173 The same above experiment obtained functionalized CNFs and pure Fe₃O₄ nanoparticles
174 without using ferric chloride, ferric sulphate and ammonia. Changing the feeding weight
175 ratios of Fe₃O₄ to CNFs (m Fe₃O₄: m CNFs = 0.1:0.1, 0.2:0.1, 0.4:0.1, 0.6:0.1, 0.8:0.1
176 and 1:0.1), gave six samples of CNFs/Fe₃O₄ nanocomposites.

177

178 **3.2. Structural Characterization of sorbent**

179 The morphology of the prepared products were investigated through a scanning electron
180 microscope (SEM) and transmission electron microscope (TEM). The SEM image of
181 synthesized CNFs on CF was shown in Fig. 1. The morphology of the fiber surface

182 showed a rough and highly porous structure which greatly increases the surface area for
183 CNF and further provide enhanced stationary phase loading and the extraction capacity.

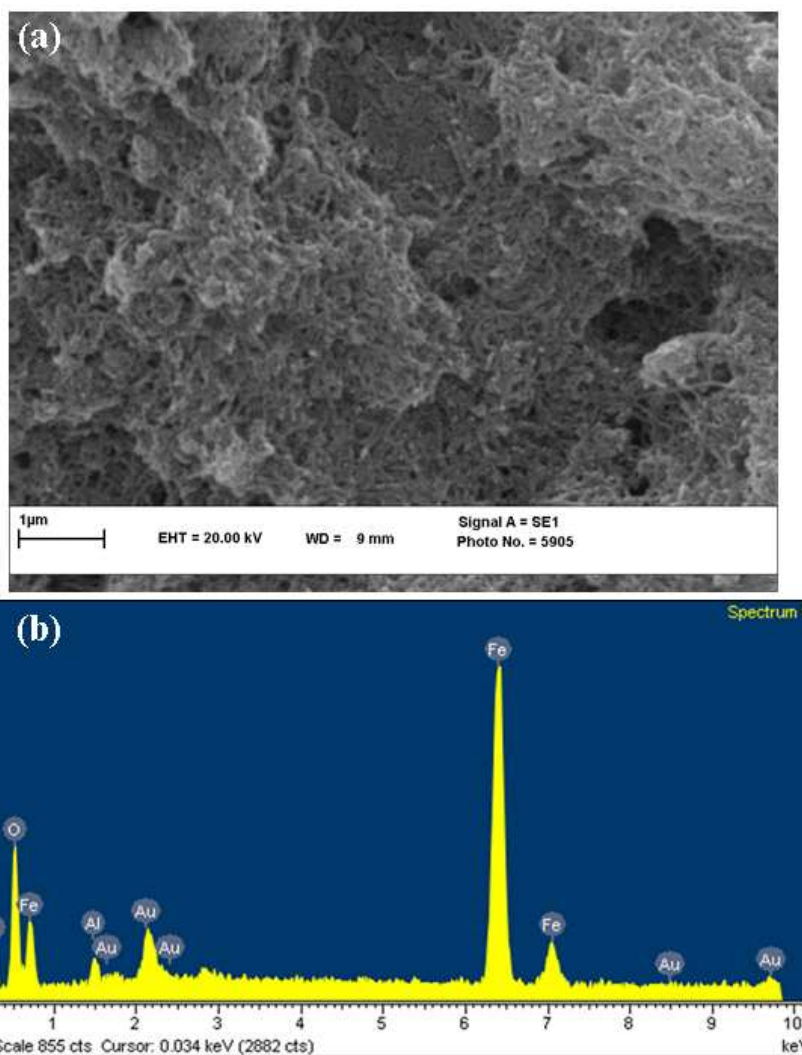


185

Fig. 1. SEM images of CNFs.

186 Also Fig. 2a display the SEM image of CNFs-Fe₃O₄, which illustrate the surface
187 morphology and uniform size distribution of Fe₃O₄ nanoparticles. One of the instruments
188 most commonly used in conjunction with the SEM is the Energy Dispersive X-ray
189 Spectrometer (EDX). Combining the EDX with the SEM allows the identification, at
190 microstructural level, of compositional gradients at grain boundaries, second phases,
191 impurities, inclusions, and small amounts of materials. In the scanning mode, the
192 SEM/EDS unit can be used to produce maps of element location, concentration, and
193 distribution. The locations of the peaks are directly related to the particular x-ray
194 "fingerprint" of the elements present. Consequently, the presence of a peak, its height,
195 and several other factors, allow the analyst to identify the elements within a sample. The

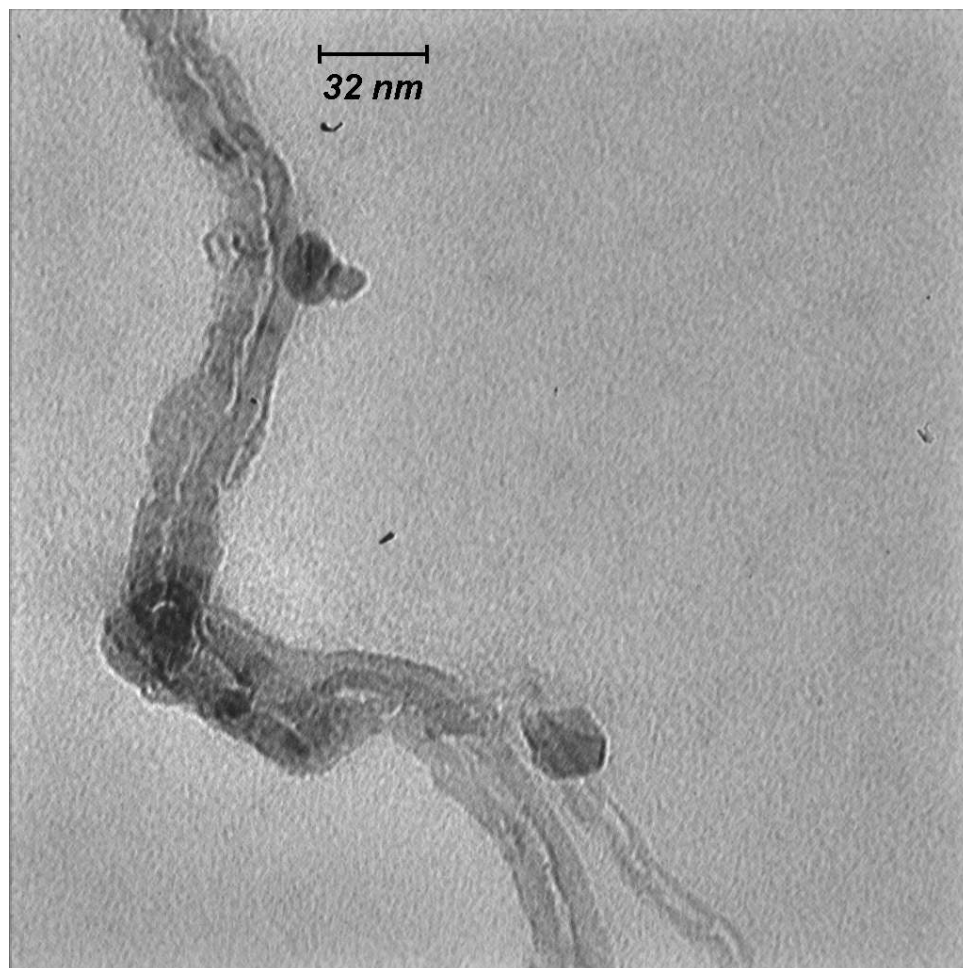
196 EDX spectra of CNFs-Fe₃O₄ nanoparticles is shown in Fig. 2b. The results confirmed the
197 existence of Fe₃O₄ nanoparticles on the CNF surface.



198

199 **Fig. 2.** (a) SEM image of CNFs-Fe₃O₄ nanoparticles, (b) EDX spectrum of CNFs-Fe₃O₄
200 nanoparticles.

201 Also, the size and morphological features of CNFs-Fe₃O₄ nanoparticles were visualized
202 with TEM. As you can see from Fig.3, the nanoparticles are spherical and have an
203 average diameter of 20 nm.



204

205

Fig. 3. TEM image of CNFs-Fe₃O₄ nanoparticles.

206

3.3. Optimization of magnetic solid-phase extraction conditions

207

In order to identify the responsible of the extraction, CNFs-Fe₃O₄ and Fe₃O₄ nanoparticles

208

were used for the MSPE of target analytes. The chromatographic peak area at the same

209

conditions and concentration for the CNFs-Fe₃O₄ and Fe₃O₄ nanoparticles were compared

210

together and results shown that the peak area for CNFs-Fe₃O₄ nanoparticles is greater

211

than Fe₃O₄ nanoparticles. This result was related to CNFs according to its special

212

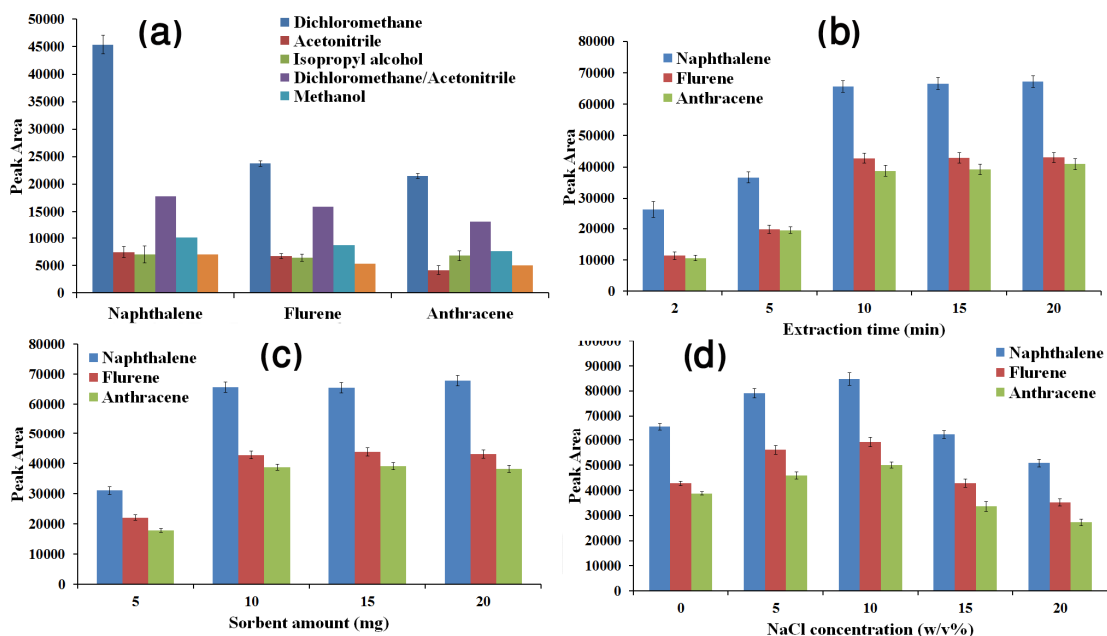
properties especially high surface area and ability to establish π - π interactions.

213 The adsorption of PAHs on different ratios of CNFs/Fe₃O₄ (m Fe₃O₄: m CNFs = 0.1:0.1,
214 0.2:0.1, 0.5:0.1, 0.6:0.1, 0.8:0.1 and 1:0.1) was recorded. The results shown that with the
215 increasing the Fe₃O₄ nanoparticles on the surface of the CNFs the adsorption capacity
216 decreased due to the surface of the CNFs was occupied by Fe₃O₄ nanoparticles. So the
217 active sites of CNFs were blocked with Fe₃O₄ nanoparticles, so the adsorption capacity
218 decreased. However, at a high amount ratios of Fe₃O₄/ CNFs, the magnetic properties of
219 adsorbent enhanced and it can easily be separated in sample solution within short time
220 under eternal magnetic field. Therefore, the Fe₃O₄/CNFs nanocomposite with the ratio
221 1:1 (m Fe₃O₄: m CNFs = 0.1:0.1) were selected for the following investigation.

222 The magnetic solid-phase extraction conditions involving the amount of sorbent,
223 adsorption and desorption times, desorption solvent and also volume, and the salt effects
224 were optimized to improve the extraction efficiency of the CNFs-Fe₃O₄. The
225 chromatographic peak area was used to evaluate the influence of the factors on the
226 extraction efficiency.

227 The selection of an appropriate desorption solvent is of major importance for the
228 optimization of MSPE process. Five solvents were tested as desorption solvent in this
229 study, including dichloromethane, acetone, isopropyl alcohol, methanol and acetonitrile.

230 As shown in Fig. 4a, desorption ability of dichloromethane was found to be higher than
231 the other solvents. Therefore, dichloromethane was used as desorption solvent throughout
232 the experiments.



233

234 **Fig. 4.** (a) Effect of eluent type on the extraction efficiency of PAHs; (b) Effect of
 235 extraction time on the extraction efficiency of PAHs; (c) Effect of c sorbent amount
 236 on the extraction recovery of PAHs (d) Effect of salt on the extraction efficiency of
 237 PAHs.

238 The desorption time was studied in the range of 0.5 to 10 min. The results showed that
 239 the time of 5 min appeared to be the optimum value for the elution of the analytes.
 240 Additionally, the effect of the eluent solution volume on the desorption efficiency of the
 241 analytes was also investigated. It was found that all the analytes could be quantitatively
 242 desorbed from the sorbent by rinsing the nano-adsorbent with 1 mL of dichloromethane.
 243 Therefore, 1 mL of dichloromethane was selected for the elution of the analytes from the
 244 nano-adsorbent.

245 Large surface area and high extraction capacity are the main advantages of nanomaterial
 246 adsorbents. Therefore, compared to micro-sized sorbents, better extraction efficiency can

247 be achieved with a less amount of NPs. To study the effect of the amount of the sorbent
248 on the extraction efficiency, the extraction was performed by varying the amounts of the
249 sorbent from 5 to 20 mg (Fig. 4b). The results demonstrated that the extraction efficiency
250 was enhanced by increasing the sorbent amount up to 10 mg. Further increase in the
251 amount of sorbent did not change significantly the analytical signals. Therefore, 10 mg of
252 the CNFs-Fe₃O₄ sorbent was used for further extractions.

253 To increase the precision and sensitivity of the extraction method, it is necessary to
254 provide an exposure time that guarantees the equilibrium between aqueous phase and
255 sorbent. For studying the effect of sorption time on extraction efficiency, sorption times
256 were varied in the range of 2.0–20 min (Fig. 4c). Due to the very high surface area to
257 volume ratios in nano-adsorbents and their short diffusion routes which lead to a high
258 rapid sorption process, the equilibrium between sample solution and sorbent surface can
259 be reached in a shorter contact time in comparison with the conventional SPE sorbents.
260 The results indicated that the extraction efficiency was enhanced by increasing the
261 sorption time from 2.0 to 10.0 min, and then remained almost constant with further
262 increase in time. Thus, the sorption time of 10.0 min was selected for further studies.

263 Addition of salt into the aqueous sample is usually causing improvement in the extraction
264 of several analytes, because the increase in ionic strength brings a reduction on the
265 solubility of the hydrophobic analytes in the water solution and forces more of these
266 analytes into the extracting phase. The increase in the extraction extent can be explained
267 by the engagement of water molecules in the hydration spheres around the ionic salt and
268 hence in the reduction of the water concentration available to dissolve analytes. The
269 salting-out effect was examined by monitoring the variation of peak areas in the presence

270 of different concentrations of NaCl (from saltless up to 20% *w/v*). Results show that the
271 extraction efficiencies of the compounds under study increased with the salt content in
272 the range tested, and in the 10% *w/v* salt concentration, maximum extraction efficiency
273 was observed (Fig. 4d) and decreases, thereafter. The negative effect is attributed to the
274 fact that the aqueous solution viscosity would increase with the addition of salt, which
275 resulted in difficult mass transfer and low extraction efficiency.

276 **3.4. Reusability of adsorbent**

277 Reusability is another important factor for evaluating the performance of the magnetic
278 nano-adsorbents. The adsorbent was regenerated by washing with 2 mL of methanol and
279 then with 5 mL water before the next MSPE application. In such way, no carry-over of
280 the analytes on the adsorbent was detected. The results showed that no obvious changes
281 were observed in the extraction efficiency after ten successive extraction process. The
282 good reusability indicates that this magnetic sorbent is stable and durable during the
283 extraction procedure.

284 **3.5. Evaluation of analytical performance**

285 Under the optimal experimental conditions, different quality parameters were evaluated
286 to assess the method performance. The results are summarized in Table 1. For the target
287 analytes quantification, the external standard calibration at eight different concentration
288 levels (for naphthalene: 0.025, 0.1, 0.5, 1, 10, 30, 50 and 100 ng mL⁻¹; fluorene: 0.04,
289 0.1, 0.5, 1, 10, 30, 50 and 100 ng mL⁻¹; anthracene: 0.08, 0.1, 0.5, 1, 10, 30, 50 and 100
290 ng mL⁻¹) was used. For each level, three replicate extractions were performed under
291 optimal conditions. Good linear relationship between the corresponding peak areas and

292 the concentrations were obtained for all the analytes ($r > 0.9965$). The limits of detection
 293 (LODs) and quantification (LOQs), based on signal-to-noise ratio (S/N) of 3:1 and 10:1,
 294 were determined. LODs and LOQs were obtained in the range of $0.008\text{--}0.03\text{ ng mL}^{-1}$ and
 295 $0.025\text{--}0.08\text{ ng mL}^{-1}$, respectively. In order to assess the repeatability of the method, five
 296 replicate determinations were carried out at three concentration levels (0.1, 10 and 100 ng
 297 mL^{-1}) and the relative standard deviations (RSDs) were calculated. The observed
 298 repeatability ranged 3.2–11.2% depending of the compound considered.

299

300 **Table 1.** Figures of merit of the proposed method for the determination of PAHs

Analyte	LOD (ng mL^{-1})	LOQ (ng mL^{-1})	Linear range (ng mL^{-1})	Correlation coefficient (r)	RSD(%) at three concentration (ng mL^{-1})		
					0.1	10	100
Naphthalene	0.008	0.025	0.025–100	0.9980	9.8	5.7	4.8
Fluorene	0.01	0.04	0.04–100	0.9965	8.4	7.4	3.2
Anthracene	0.03	0.08	0.08–100	0.9965	11.2	4.6	4.5

301

302 **3.6. Real sample analysis**

303 To evaluate the applicability of the proposed method, extraction and analysis was
 304 performed on different water matrices such as tap water, river water, well water and
 305 waste water samples. The quantitative results of this water samples are listed in Table 2.
 306 In order to investigate the performance of the established method, CNFs- Fe_3O_4 sorbents
 307 was applied to extract these water samples spiked at three concentration levels (0.1, 10
 308 and 100 ng mL^{-1}) for each compound. The recoveries and determination precisions are
 309 listed in Table 2. The results showed that the mean recoveries of PAHs ($n = 3$) ranged

310 from 90.1 to 100.9% and the RSDs were between 3.2% and 9.8%. These results clearly
 311 demonstrated that the matrix effect did not have a significant role on the extraction
 312 efficiency. Fig. 5 shows the GC chromatograms obtained from spiked wastewater
 313 samples at concentration level of 10 ng mL⁻¹ with the CNFs-Fe₃O₄. Downward shift in
 314 background of chromatogram may be due to some impurities in the background which
 315 are very volatile and coming up very soon in low temperature, and by increasing the
 316 temperature the baseline become stable.

317 **Table 2.** Content of PAHs in different water samples and the accuracy of the established proposed
 318 method.

Sample	Analyte	Mean (ng mL ⁻¹)	Spiked amount (ng mL ⁻¹)					
			0.1		10		100	
			Relative recovery (%) ^a	RSD (%)	Relative recovery (%) ^a	RSD (%)	Relative recovery (%) ^a	RSD (%)
Tap water	Naphthalene	ND	95.6	9.8	99.0	5.2	98.6	4.5
	Fluorene	ND	98.2	5.8	99.1	5.1	97.8	5.0
	Anthracene	ND	96.4	6.2	97.3	5.1	99.0	4.1
Well water	Naphthalene	ND	94.8	7.5	96.2	5.9	100.9	5.1
	Fluorene	ND	93.9	5.4	93.0	4.8	97.6	3.2
	Anthracene	ND	95.7	5.9	96.5	5.3	98.3	4.7
River water	Naphthalene	ND	93.7	7.5	96.9	6.3	98.1	6.5
	Fluorene	ND	96.3	8.9	98.6	5.6	95.8	4.9
	Anthracene	0.085	97.1	9.1	97.5	7.7	98.0	5.8
Wastewater	Naphthalene	0.038	92.3	8.6	93.9	6.0	93.5	6.5
	Fluorene	ND	93.7	5.5	95.0	4.5	95.9	4.6
	Anthracene	ND	90.1	7.1	91.6	5.9	92.1	6.4

319 ND: not detected

320 ^a: Relative recovery (%)= (The found amount in the spiked sample – The found amount in the
 321 sample/The added amount) × 100.

322

323

324

325

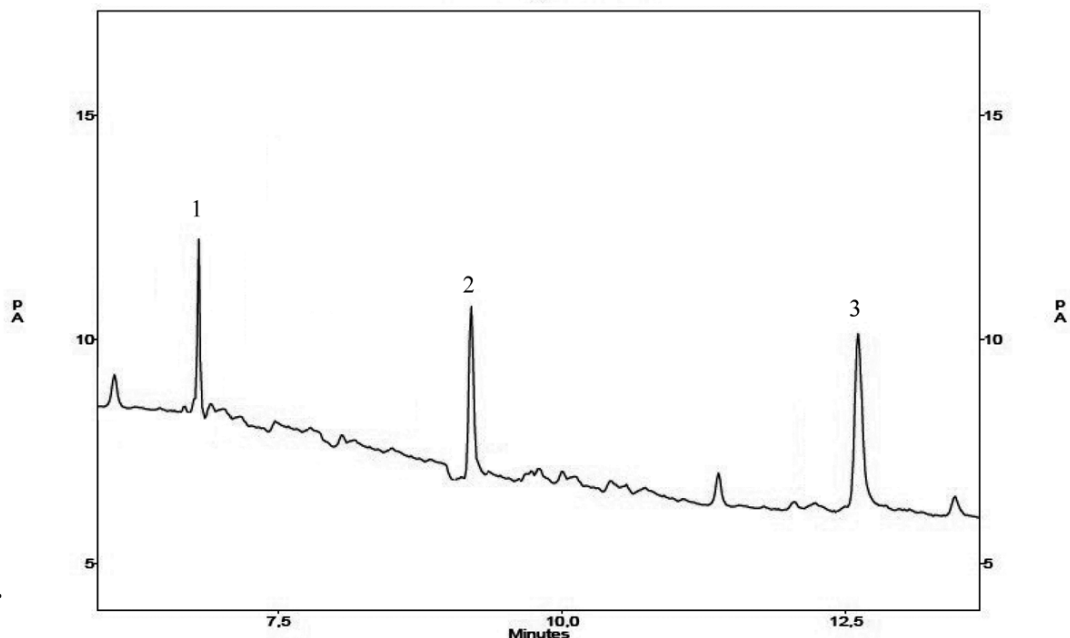
326

327

328

329

330

331 **Fig.**

332 peaks: (1) Naphthalene, (2) Fluorene and (3) Anthracene.

333

334 **3.7. Comparison with other related methods**

335 A comparison between the figures of merit of the proposed method and some of the

336 reported methods for the extraction and determination of PAHs water samples are

337 summarized in Table 3.^{19–23} The comparison of the results with other reported methods

338 revealed that the proposed method has wider linear dynamic range and lower detection

339 limit. Also, due to the large surface area and rapid extraction dynamics of the MNPs, this

340 method has a very short extraction time using small amount of organic solvent. Hence,

341 the analytical performance of the current method is acceptable.

342

343

344

345

346 **Table 3.** Comparison of the proposed method with other methods applied for the
 347 extraction and determination of PAHs.

Method	Analytes	Sample	LOD (ng mL ⁻¹)	Linear range (ng mL ⁻¹)	RSD (%)	Reference
DLLME-SFO-HPLC	Naphthalene, acenaphthene, anthracene, fluoranthene	Water	0.045–1.10	0.1–50	1.3–4.4	21
LPME-SFO-GC-FID	Phenanthrene, anthracene, fluoranthene, pyrene, benz[<i>a</i>]anthracene, chrysene, benzo[<i>b</i>]fluoranthene, benzo[<i>k</i>]fluoranthene, benzo[<i>a</i>]pyrene, dibenz[<i>ah</i>]anthracene, indeno[123- <i>cd</i>]pyrene, benzo[<i>ghi</i>]perylene	Water	0.07–1.67	0.25–300	<7	22
SPME-GC-FID	Acenaphthylene, fluoranthene, fluorene, naphthalene, phenanthrene, biphenyl	Water	0.04–0.06	0.1–100	4.1–6.7	23
SPME-GC-FID	Naphthalene, acenaphthylene, fluorene, phenanthrene, anthracene, fluoranthene, pyrene, biphenyl	Water	0.02–0.08	0.1–300	5.4–7.8	24
SPME-GC-FID	Naphthalene, acenaphthene, acenaphthylene, fluorene, phenanthrene, anthracene, fluoranthene, pyrene, benz[<i>a</i>]anthracene, chrysene, benzo[<i>b</i>]fluoranthene, benzo[<i>k</i>]fluoranthene, benzo[<i>a</i>]pyrene, indeno(1,2,3- <i>cd</i>)pyrene, dibenz[<i>a,h</i>]anthracene, benzo[<i>-ghi</i>]perylene	Water	0.03–0.1	0.1–100	6–9	25
SPME-GC-FID	Naphthalene, phenanthrene, anthracene, fluoranthene, pyrene	Water and smoked rice	0.009–0.013	0.02–1000	1.33–3.61	26
SPE-HPLC-FD	Fluorene, anthracene, fluoranthene, pyrene, 1,2-benzanthracene, benzo[<i>b</i>]fluoranthene, benzo[<i>k</i>]fluoranthene	Water	0.0008–0.016	0.001–2.4	2.9–3.3	27
MSPE-GC-FID	Naphthalene, fluorene, anthracene.	Water	0.008–0.03	0.025–100	3.2–11.2	This study

348 **Abbreviations:** DLLME, Dispersive liquid–liquid microextraction; HPLC, High
 349 performance liquid chromatography; LPME-SFO, Liquid-phase microextraction method
 350 based on the solidification of a floating organic microdrop; SPME, Solid-phase
 351 microextraction.

352 4. Conclusion

353 In this work, for the first time, carbon nanofibers-Fe₃O₄ sorbents were prepared and then
 354 successfully applied for the analysis of some of polycyclic aromatic hydrocarbons in real
 355 water samples. Due to the unique properties of carbon nanofibers and the inherent
 356 advantageous features, this innovative sorbent exhibited porous surface structure, wide
 357 linearity, satisfactory relative recovery, good sensitivity and precision and short analysis

358 time. Additionally, this technique was successfully utilized to analyze of polycyclic
359 aromatic hydrocarbons in real water samples with satisfactory accuracy and precision. On
360 the basis of the obtained results, it is anticipated that the proposed method has a great
361 analytical potential in the preconcentration of trace analytes from real sample in the same
362 way.

363 **Acknowledgment**

364 The authors are thankful to Ferdowsi University of Mashhad, Iran, for financial support
365 of this work.

366 **References**

- 367 1 O.P. Heemken, N. Theobald and B.W. Wenclawiak, *Anal. Chem.*, 1997, **69**, 2171–
368 2180.
- 369 2 R.-A. Doong, S.-M. Chang and Y.-C. Sun, *J. Chromatogr. A*, 2000, **879**, 177–188.
- 370 3 P.K. Wong and J. Wang, *Environ. Pollut.*, 2001, **112**, 407–415.
- 371 4 European Commission (2002) Opinion of the Scientific Committee on Food.
372 http://ec.europa.eu/food/fs/sc/scf/out153_en.pdf
373
- 374 5 USEPA (1986) Method 8310 polynuclear aromatic hydrocarbons. In USEPA (Ed.),
375 EPA test methods SW-846 on-line (Vol. 2008)
- 376 6 P. Popp, C. Bauer, M. Moder and A. Paschke, *J. Chromatogr. A*, 2000, **897**, 153–159.

- 377 7 S. K. Pandey, K.-H. Kim and R. J. C. Brown, *Trends Anal. Chem.*, 2011, **30**, 1716–
378 1739.
- 379 8 C. F. Poole, A. D. Gunatilleka and R. Sethuraman, *J. Chromatogr. A*, 2000, **885**, 17–39.
- 380 9 G. Giakisikli and A. N. Anthemidis, *Anal. Chim. Acta*, 2013, **789**, 1–16.
- 381 10 M. Wierucka and M. Biziuk, *Trends Anal. Chem.*, 2014, **59**, 50–58.
- 382 11 Q. Gao, D. Luo, J. Ding and Y.Q. Feng, *J. Chromatogr. A*, 2010, **1217**, 5602–5609.
- 383 12 R. Lucena, B.M. Simonet, S. Cárdenas and M. Valcárcel, *J. Chromatogr. A*, 2011,
384 **1218**, 620–637.
- 385 13 E. M. Reyes-Gallardo, R. Lucena, S. Cárdenas and M. Valcárcel, *J. Chromatogr. A*,
386 2014, **1345**, 43–49.
- 387 14 K. Scida, P. W. Stege, G. Haby, G. A. Messina and C. D. García, *Anal. Chim. Acta*,
388 2011, **691**, 6–17.
- 389 15 F. Ghaemi, A. Amiri and R. Yunus, *Trends Anal. Chem.*, 2014, **59**, 133–143.
- 390 16 L. Zhang, A. Aboagye, A. Kelkar, C. Lai and H. Fong, *J. Mater. Sci.*, 2014, **49**, 463–
391 480.
- 392 17 P. A. Tran, L. Zhang and T. J. Webster, *Adv. Drug Deliver. Rev.*, 2009, **61**, 1097–
393 1114.

- 394 18 N. M. Rodriguez, A. Chambers and R. T. K. Baker, *Langmuir*, 1995, **11**, 3862–3866.
- 395 19 S. Chigome, G. Darko and N. Torto, *Analyst*, 2011, **136**, 2879–2889.
- 396 20 P. V. Lakshminarayanan, H. Toghiani and C. U. Pittman Jr, *Carbon*, 2004, **42**, 2433–
397 2442.
- 398 21 H. Xu, Z.Q. Ding, L.L. Lv, D.D. Song and Y.-Q. Feng, *Anal. Chim. Acta*, 2009, **636**,
399 28–33.
- 400 22 M.R.K. Zanjani, Y. Yamini, S. Shariati and J.A. Jonsson, *Anal. Chim. Acta*, 2007,
401 **585**, 286–293.
- 402 23 S. Maghsoudi and E. Noroozian, *Chromatographia*, 2012, **75**, 913–921.
- 403 24 M. Behzadi, E. Noroozian and M. Mirzaei, *Talanta*, 2013, **108**, 66–73.
- 404 25 M.-C. Wei and J. Jen, *Talanta*, 2007, **72**, 1269–1274.
- 405 26 A.A. Matin, P. Biparva and M. Gheshlaghi, *J. Chromatogr. A*, 2014, **1374**, 50–57.
- 406 27 H. Hu, S. Liu, C. Chen, J. Wang, Y. Zou, L. Lin and Shouzhuo Yao, *Analyst*,
407 2014, **139**, 5818–5826.
- 408
- 409
- 410
- 411
- 412

413 **Figure Captions**

414 **Fig. 1.** SEM images of CNFs.

415 **Fig. 2.** (a) SEM image of CNFs-Fe₃O₄ nanoparticles, (b) EDX spectrum of CNFs-Fe₃O₄
416 nanoparticles.

417 **Fig. 3.** TEM image of CNFs-Fe₃O₄ nanoparticles.

418 **Fig. 4.** (a) Effect of eluent type on the extraction efficiency of PAHs; (b) Effect of
419 extraction time on the extraction efficiency of PAHs; (c) Effect of sorbent amount
420 on the extraction recovery of PAHs (d) Effect of salt on the extraction efficiency of
421 PAHs.

422 **Fig. 5.** GC chromatogram of wastewater sample spiked at 10 ng mL⁻¹. Chromatographic
423 peaks: (1) Naphthalene, (2) Fluorene and (3) Anthracene.

424

425

426 **Table Captions**

427 **Table 1.** Figures of merit of the proposed method for the determination of PAHs.

428 **Table 2.** Content of PAHs in different water samples and the accuracy of the established
429 proposed method.

430 **Table 3.** Comparison of the proposed method with other methods applied for the
431 extraction and determination of PAHs.